Lattice dynamics of boron phosphide

1992 J. Phys.: Condens. Matter 4 6603

(http://iopscience.iop.org/0953-8984/4/31/012)

J. Phys.: Condens. Matter 4 (1992) 6603–6612. Printed in the UK

Lattice dynamics of boron phosphide

H W Leite Alves† and K Kunc

Laboratoire de Physique des Solides associé au CNRS, Université Pierre et Marie Curie, 4 place Jussieu, Tour 13, 75252 Paris Cédex 05, France

Received 19 March 1992

Abstract. Using the density-functional theory, norm-conserving pseudopotentials and plane-wave expansions, we have calculated *ab initio* the equation of state and the principal phonon modes in boron phosphide, including their pressure dependence and the amplitude of the eigendisplacements. Good agreement with experiment is obtained, whenever a comparison is possible: in fact, most of the results are predictions. A ten-parameter valence overlap shell model is then constructed from the available experimental data, which are completed by the data obtained in the first-principle calculations: frozen-phonon frequencies and eigenvectors. The previous speculations about the anomalous behaviour of the effective charges are discussed in the context of the present results.

1. Introduction

There has been considerable interest in the physical properties of boron phosphide (BP) since its hardness, high melting point and resistance to corrosion were noticed [1]. The compound is a promising material for use in optoelectronic and microelectronic devices working under difficult conditions such as high temperatures or aggressive environments [2]. The amount of theoretical knowledge on this substance is, unfortunately, limited to a handful of studies [3–5] and, in particular, the data on phonon spectra and vibrational properties are rather scarce [6, 7].

Under normal conditions, BP appears in a zincblende structure and shows an indirect Γ–X gap of 2.4 eV. According to the recent total energy calculations [4], it undergoes at a hydrostatic pressure of 160 GPa a phase transition to the rocksalt structure which is semimetallic. The β-Sn modification, which one would expect to be the high-pressure structure from simple ionicity and heteropolarity arguments or by analogy with the calculated phase diagrams of other III–V compounds, turns out to be less energetically favourable than the rocksalt modification.

The calculations in [3] also revealed that the calculated charge distribution differs from the usual III–V picture characterized by a large accumulation of the electronic charge around the anion: in BP the strongly attractive B potential causes a nearly symmetrical distribution of the valence charge between the cation and the anion, reminiscent of homopolar bonding; the small heteropolarity is thus a consequence of the strong electronegativity of the B atoms. It was also noticed [4] that at high pressures this homopolarity is enhanced. According to experiment [7], the transverse

† On leave from: Departamento de Física dos Materiais e Mecânica, Instituto de Física, Universidade de São Paulo, CP 20516, CEP 01498, São Paulo, Brazil.

0953-8984/92/316603+10$04.50

effective charges e_T^* associated with the atoms decrease with increasing pressure. Despite the fact that the experiment is not capable of precise determination of the sign of e_T^*, Sanjurjo *et al* [7] deduced, from the evaluation of the pseudopotential form factors, that this sign ($e_T^*(B)$) is negative since the polarity of BP is close to zero.

As the electronic and structural properties of BP have already been addressed [3, 4] within the density-functional theory [8] in the local-density approximation (LDA), we have applied the same approach to calculate the total energy in order to supply the missing experimental information on the vibrational properties of BP in the zincblende modification. Norm-conserving pseudopotentials [9] are used, together with plane-wave expansions, and the Ceperley–Alder exchange–correlation [10] is adopted. Following the procedures summarized for example in [11] we start by checking the lattice parameter a_0, bulk modulus B_0 and its pressure derivative B_0', as well as the electronic charge distribution $n(\mathbf{r})$ in section 2, and calculate the frequencies and eigenvectors of selected phonons in section 3. A construction of a simple mechanical model (valence overlap shell model (VOSM)) [12] is then attempted in section 4, which accounts, in terms of ten parameters, for all the calculated frequencies *and* eigenvectors, as well as for all the available experimental data (such as the elastic constants, and the TO(Γ) and LO(Γ) frequencies). The question of the sign of the effective charges of B and P is raised and briefly discussed in section 5. The main results are summarized in section 6.

2. Equilibrium properties

Our first step consists in verifying that our calculational procedure correctly describes the undistorted structure in static equilibrium. We have evaluated the total energy for various values of the lattice constant, at different plane-wave energy cut-offs and numbers of k-points sampled in the irreducible Brillouin zone (BZ). The results were fitted by the Murnaghan equation of state and the convergence of the calculated static properties is summarized in table 1, for cut-off energies E_{pw} varying from 12 to 27 Ryd.

Table 1. Convergence of the calculated static properties of zincblende BP with energy cut-offs of the plane-wave expansion and with the number of k-points in the BZ sampling.

E_{pw} (Ryd)	Number of k-points	a_0 (Å)	B_0 (Mbar)	B_0'
12	2	4.860	0.33	6.11
15	2	4.574	1.80	3.11
18	2	4.549	1.71	3.17
21	2	4.530	1.82	2.74
24	2	4.522	1.65	3.33
27	2	4.514	1.72	3.14
12	10	4.652	1.61	2.94
15	10	4.574	1.82	3.12
18	10	4.543	1.68	3.29
21	10	4.526	1.70	3.22
24	10	4.517	1.67	3.28
Experiment		4.538	1.73 [13] 2.67 [14]	

The results obtained for the lattice constant ($a_0 = 4.52$ Å), bulk modulus ($B_0 = 1.67$ Mbar) and its pressure derivative ($B_0 = 3.3$) are in good agreement with the available experimental results [13, 14] (error of 0.5–3.5%), as well as with the previous calculations [3] in which $a_0 = 4.56$ Å and $B_0 = 1.65$ Mbar were obtained. We also verified that our calculated LDA band structure agrees with that found in [3]; our calculated full valence band width of 15.7 eV and direct gap of 3.34 eV compare well with the values of 15.3 eV and 3.3 eV from [3]. We also obtained an indirect gap of 1.01 eV at $\Delta_{\min} = (2\pi/a_0)(0,0,0.84)$ which is close to the value of 1.2 eV found in the previous calculations [3].

The real-space distribution of the electronic charge density $n(r)$ shown in figure 1 agrees with the previous calculations [3] as well: it is immediately apparent from the contour plot that the valence charge distribution of BP differs considerably from that of typical III–V semiconductors [15], in that it shows a significant bond charge between the atoms, which suggests the idea of a covalent rather than an ionic bonding.

3. Frozen phonons

The phonon frequencies and the respective eigenvectors of the vibrations at the high-symmetry points in the BZ were calculated by the well known 'frozen-phonon' method [11]: the frequency of the phonon is obtained from the difference between the total energies of the undisplaced structure and the structure with atoms displaced in the particular phonon mode. In this way, we evaluated the eigenfrequencies and eigenvectors of the TO(Γ), LO(X), LA(X), TO(X), TA(X), LO(L) and LA(L) phonons. For most of the zone-boundary phonons, one also has to determine the actual displacement patterns; the procedure will be described later and the results are summarized in table 2.

The *ab initio* calculations have much to offer in this area since very little experimental work exists for this material. The only data that can be compared with our calculations are the phonon frequency ν and the Grüneisen parameter γ for the TO mode at Γ obtained by Raman measurements [7] which are, respectively, 23.95 THz and 1.3, and with which our calculated values, 24.25 THz and 1.14, agree to within +4% and −12%, respectively.

Another way to obtain the TO(Γ) phonon frequency is to consider a tetragonal double cell—the same as is used in the subsequent calculation of the phonons at X—and to impose the displacement pattern shown in figure 2. Although one has to deal with a cell twice as large as the usual trigonal cell, the strong cubic anharmonicity does not appear now and one does not need to calculate ΔE^{tot} twice (with $+u$ and $-u$) to eliminate that contribution [16]. The convergence test of evaluation of the TO(Γ) phonon frequency is shown in figure 3.

To calculate the longitudinal phonons, one considers the same tetragonal double cell (see e.g. [16]), and the displacement patterns consist of oscillations of either the B or the P sublattices alone [16]. The difference between the masses of B and P is so large that even without the energy calculations we can identify the LO mode with the displacements of the B sublattice (the lighter atoms) and the LA mode with the P-atom oscillations. These displacement patterns were, indeed, confirmed by our calculations in the same way as they were verified earlier for GaP [17].

For the transverse phonons at X and for the phonon modes at L we know that we can treat these modes as coupled oscillations of displacement patterns S_1 and

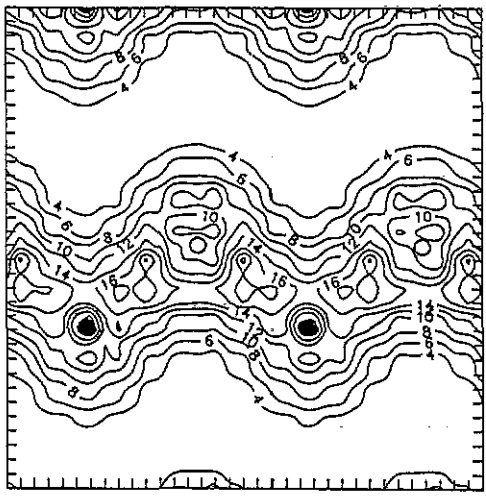

Figure 1. Pseudo-charge density for zincblende BP in static equilibrium calculated in the (110) plane. The unit of length is the lattice constant a and the contour interval is 2 electrons/cell. The full circles are the B atoms while the open circles are the P atoms.

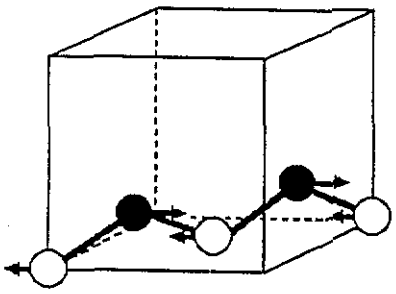

Figure 2. Displacement pattern used in the determination of the TO(Γ) mode in the alternative double-cell calculations.

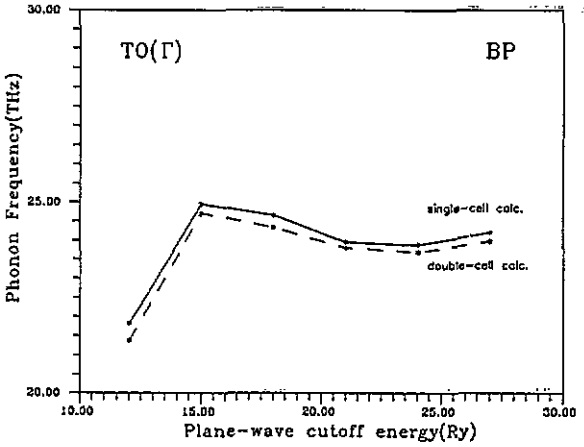

Figure 3. Convergence of the *ab initio* calculation of the TO(Γ) phonon frequency with the cut-off energy of the plane waves. The full curves correspond to the single-cell calculations and the broken curves to the double-cell calculations with the displacement pattern shown in figure 2.

S_2 which correspond to the respective phonon modes in the diamond structure. We proceed, then, as in the previous work [18, 19] and evaluate the correct linear combination of these displacement patterns by diagonalizing the 2×2 matrices of the coupling coefficients. In contrast with [19], we used for evaluation of the modes at L the unit cells defined by the translational vectors $a_1 = a_0(0, 0.5, -0.5)$, $a_2 = a_0(-0.5, 0.5, 0)$, $a_3 = a_0(1, 1, 0)$. The convergence of the calculated frequencies of

the zone-boundary phonons (LO(X), LA(X), TO(X), TA(X), LO(L) and LA(L)) with the plane-wave energy cut-off is shown in figures 4 and 5; their frequencies and Grüneisen parameters are summarized in table 2.

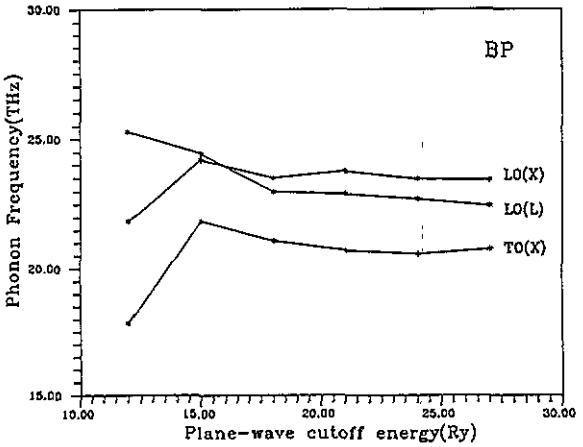

Figure 4. Convergence of the *ab initio* calculations of the optical phonon frequencies at the X and L points of the BZ with the cut-off energy of the plane waves.

Table 2. Summary of the most important phonon frequencies with their respective Grüneisen parameters γ calculated *ab initio*. The results given here were obtained with the cut-off energy of 21 Ryd in the plane-wave expansions.

Phonon mode	ν (THz)	γ	Number of k-points
TO(Γ)	24.25	1.14	5
LO(X)	24.00	0.90	3
LA(X)	15.81	0.94	3
TO(X)	21.04	1.54	4
TA(X)	9.20	−0.27	4
LO(L)	22.91	1.03	12
LA(L)	15.18	1.00	12
Experiment TO(Γ)	23.95	1.3	[7]

There are no experimental data for these modes in BP and our calculations present an attempt to supply the missing information. We observe that, as in other III–V compounds, the TA(X) is a soft mode and its frequency decreases with increasing pressure; the Grüneisen parameter γ has a negative value.

When the problem of coupled oscillations S_1 and S_2 is solved [18, 19], the resulting linear combination of the displacement patterns provides us with information about the eigenvectors of each vibrational mode. The eigenvectors, described by the atomic displacement ratio u_1/u_2 (the subscript 1 refers to B, and the subscript 2 to P), tell us about the amount of coupling between the generalized coordinates S_1 and S_2 defined above. For the transverse phonons at X, and unlike the situation for GaAs, the u_1/u_2 ratio is not close to 1 [16], a consequence of the larger difference

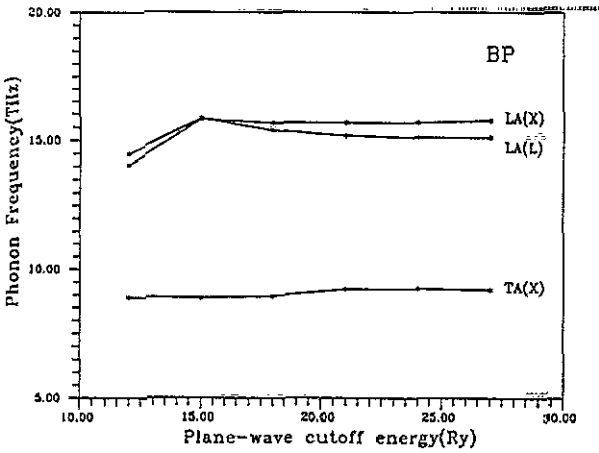

Figure 5. Convergence of the *ab initio* calculations of the acoustic phonon frequencies at the X and L points of the BZ with the cut-off energy of the plane waves.

between the cation and anion masses. We obtained $u_1/u_2 \simeq 0.8$ for TA(X) and $u_1/u_2 \simeq -3.6$ for TO(X); similar values differing from approximately 1 were also obtained for GaP [17] and for SiC [18].

Another observation concerns the eigenvectors of the LO(L) and LA(L) phonon modes; the calculated $|u_1/u_2|$ ratios approach the values which mean, practically, ∞ and 0—although no symmetry argument requires one sublattice to vibrate and the other to be at rest. We note that a similar result was obtained for SiC [19] as well and is probably due to the large difference between the masses of the two atoms. All calculated values of the eigenvectors are given later in the last column of table 4.

4. Shell model

The most widely used among the different mechanical models of interatomic interaction in semiconductor compounds has been the well known shell model of Dick and Overhauser [20] and Cochran [21]. In this model, the ions are assumed to be polarizable and mechanically deformable and the atomic vibrations are described as the motion of a system of *cores* and massless charged *shells*, bound to the respective *cores* by harmonic springs; the *cores* are connected to each other, in the most general case, by tensor forces. The vibrations then cause polarization and deformation of the electronic charge distribution in a crystal, which is modelled as relative displacements of the shells.

The particular version of the shell model that we use is known as VOSM [12]; all the generalized forces are assumed to have the form of a 'valence force field'. In this work, the ten model parameters were fitted, by a non-linear least-squares method with constrained parameters and weighting, to all the available information about phonon frequencies, elastic constants and eigenvectors at X and L. In other words, to the set of phonon frequencies evaluated by the frozen-phonon method in the previous section, we are adding the experimental values of the TO(Γ) and LO(Γ) frequencies and of the elastic constants c_{11}, c_{12} and c_{44}. In addition, we have also included in the minimized sum of squares the data on the eigendisplacements, i.e., the ratio u_1/u_2

of the amplitudes for the transverse modes at X and the longitudinal modes at L, as well as the information on which the sublattice moves in the longitudinal modes at X. The fitting process follows closely the procedure developed in [19] in which the same ideas were applied to SiC.

The initial guess for the ten parameters was obtained using the existing parameters for GaP [12], changing only the mass of the cation and the lattice constant (mass approximation). The elastic constants were accounted for through the phonon frequencies at $k = (2\pi/a_0)(0.03,0,0),(2\pi/a_0)(0.03,0.03,0)$ and $(2\pi/a_0)(0.03,0.03,0.03)$, predicted by the elasticity theory. As experienced already by Cheng *et al* [19], the most satisfactory results are obtained with heavy weighting of the data near Γ (i.e. the elastic constants), and of the eigenvectors for the transverse modes at X. In table 3 we summarize the model parameters obtained by the fitting procedure: the initial set of parameters (row (a)) and the final set (row (b)); the resulting frequencies and displacements are shown in table 4 and in figure 6. The calculated phonon dispersion (figure 6) shows the same general features as for other III–V semiconductor compounds [22].

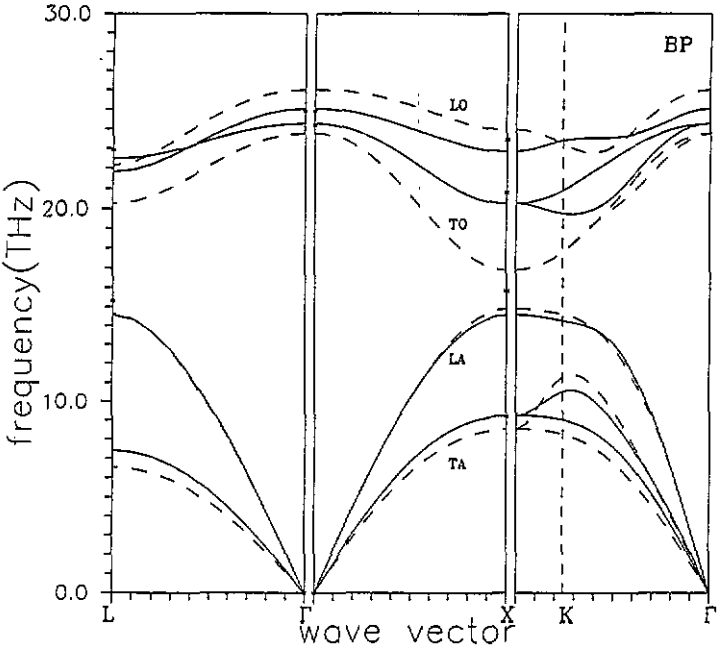

Figure 6. Phonon dispersion curves of zincblende BP calculated by VOSM. The broken curves correspond to the initial guess and the full curves were obtained from the final set of parameters (row (b) in table 3). The asterisks indicate the experimental and the *ab initio* results.

In table 4, the phonon frequencies and eigendisplacements at the high-symmetry points calculated by the VOSM are compared with those obtained in the *ab initio* calculations, as well as with the experimental values, whenever available. The final results show, in general, good agreement in frequencies (deviation of 5%); as for the displacements, we note that, despite their inclusion in the fitting procedure, the eigenvectors of the TO(X) phonon and also of the LO(L) and LA(L) phonons are only

Table 3. Parameters of the VOSM for BP: row (a), the initial guess obtained by the mass approximation on the parameters of GaP [12]; row (b), the final set of parameters. All parameters are in e^2/v_a units, with $v_a = a^3/4$ and $a = 4.52$ Å, except the charges Z_1, Y_1 and Y_2 which are in atomic units.

	λ	k_θ	k'_θ	$k_{r\theta}$	$k'_{r\theta}$	Z_1	Y_1	Y_2	K_1	K_2
(a)	47.5	−1.15	−0.31	4.61	−7.06	2.00	6.03	−1.87	371.2	82.00
(b)	46.2	0.88	−2.07	4.95	−7.50	2.14	5.15	−2.97	296.9	80.81

Table 4. Phonon frequencies and eigendisplacements at high-symmetry points of the BZ calculated by the VOSM with the parameters listed in table 3.

	Table 3, row (a)		Table 3, row (b)		LDF calculation		Experiment [7]
	ν (THz)	$\lvert u(B)/u(P)\rvert$	ν (THz)	$\lvert u(B)/u(P)\rvert$	ν (THz)	$\lvert u(B)/u(P)\rvert$	ν (THz)
LO(Γ)	26.00	2.87	25.04	1.24			24.90
TO(Γ)	23.76	2.87	24.28	1.24	24.25		23.95
LO(X)	23.94	∞	22.83	∞	24.00	∞	
LA(X)	14.90	0	14.57	0	15.81	0	
TO(X)	16.90	0.92	20.27	2.52	21.04	3.59	
TA(X)	8.53	0.94	9.25	0.81	9.20	0.80	
LO(L)	22.12	109.88	21.81	11.01	22.91	94.51	
LA(L)	14.66	0.03	14.58	0.26	15.18	0.03	
TO(L)	20.27	0.85	22.46	2.58			
TA(L)	6.54	0.83	7.40	0.70			

imperfectly reproduced. The calculated elastic constants ($c_{11} = 31.33 \times 10^{11}$ dyn cm^{-2}, $c_{12} = 10.26 \times 10^{11}$ dyn cm^{-2} and $c_{44} = 15.39 \times 10^{11}$ dyn cm^{-2}) agree with the experimental values [14] to within about 4%.

5. Effective charges

As we have seen in the previous sections, the electronic charge distribution in BP differs from those in the usual III–V compounds because the density is nearly symmetrically distributed between the cation and the anion. In view of the strong electronegativity of the B atoms, speculations arose about the *sign* of the effective charges in BP, which are determined by Raman spectroscopy or infrared absorption only in absolute value; it was suggested [7] that, contrary to the usual 'polarity', the effective charges of B might be negative and those of P positive.

We thus attempted to evaluate the effective charges *ab initio*, by proceeding exactly as in [11]; we used a tetragonal cell of BP which was six times the size of the primitive cell (volume, $6a^3/4$), and accomplished three self-consistent calculations: one with all the atoms in their equilibrium position and two with only one atomic plane (B or P) displaced by $u = 0.005a_0(1,0,0)$. The screening Hartree potential was averaged in the planes perpendicular to the [100] direction, and from the slope of its variation with x we obtained the longitudinal effective charge e^*_L. On the other hand, from the Hellmann–Feynman forces acting on the atoms in the centre of the supercell, we calculated the transverse effective charge e^*_T; the method is discussed in much detail in [11, 23].

Most of our attempts were restricted to calculations with a cut-off energy of 12 Ryd and three 'special k-points' sampling of the BZ, and we do not consider them sufficiently converged to provide reliable absolute values of e_L^* and e_T^*. Nevertheless, all calculations revealed that the effective charges are weaker and show *the same signs* as in GaAs, i.e. $e^*(B) > 0$ and $e^*(P) < 0$.

The speculations about the anomalous sign of the effective charges are thus *not* confirmed. Further calculations are required which would also provide the absolute values of the charges and, in particular, their behaviour with pressure.

6. Conclusion

We have studied the lattice dynamics of BP using the density-functional theory, norm-conserving pseudopotentials and plane-wave expansions. This procedure describes correctly the undistorted structure of BP in static equilibrium, and our results for the lattice constant and bulk modulus are in good agreement with the available experimental results.

Having a good description of the static equilibrium of BP, we have calculated *ab initio* its phonon frequencies and eigenvectors at high-symmetry points at the BZ. At the Γ point of the BZ, our results agree well with those obtained by Raman scattering [7]. At the X and L points of the BZ, our calculated data are predictions and are meant to supply the missing experimental information.

Finally, we fitted all the available information by a ten-parameter VOSM and obtained the complete phonon dispersion curves in terms of this interpolation scheme. The calculated elastic constants agree with the experimental value within about 4%.

Our attempts at evaluation of the effective charges have shown that the longitudinal effective charges are fairly small and did not confirm the speculations about the signs; for both e_L^* and e_T^* we obtained $e^*(B) > 0$ and $e^*(P) < 0$.

Acknowledgments

We wish to express our thanks to A T Lino, A Muñoz and N Meskini for useful discussions in the course of this work. The computer resources were provided by the Scientific Committee of the Centre de Calcul Vectoriel pour la Recherche. One of us (HWLA) wishes to thank the Conselho Nacional de Desenvolvimento Científico e Tecnológico, Brazil, for financially supporting his stay in Paris.

References

[1] Golikova O A 1979 *Phys. Status Solidi* a **51** 11
[2] Kumashiro Y 1990 *J. Mater. Res.* 5 2933
[3] Wentzcovitch R M, Chang K J and Cohen M L 1986 *Phys. Rev.* B **34** 1071
[4] Wentzcovitch R M, Cohen M L and Lam P K 1987 *Phys. Rev.* B **36** 6058
[5] Orlando R, Dovesi R, Roetti C and Saunders V R 1990 *J. Phys.: Condens. Matter* **2** 7769
[6] *Landolt–Börnstein New Series: Numerical Data and Functional Relationships in Science and Technology 1982* vol 17a, ed O Madelung (Berlin: Springer)
Landolt–Börnstein New Series: Numerical Data and Functional Relationships in Science and Technology 1989 vol 22a, ed O Madelung (Berlin: Springer)
[7] Sanjurjo J A, López-Cruz E, Vogl P and Cardona M 1983 *Phys. Rev.* B **28** 4579

[8] Hohenberg P and Kohn W 1964 *Phys. Rev.* **136** B864
Kohn W and Sham L J 1965 *Phys. Rev.* **140** A1133
Sham L J and Kohn W 1966 *Phys. Rev.* **145** B561
[9] Bachelet G B, Hamann D R and Schlüter M 1982 *Phys. Rev.* B **26** 2314
[10] Ceperley D M and Alder B I 1980 *Phys. Rev. Lett.* **45** 566
Perdew J and Zunger A 1981 *Phys. Rev.* B **23** 5048
[11] Kunc K 1985 *Electronic Structure, Dynamics and Quantum Structural Properties of Condensed Matter* ed J T Devreese and P E van Camp (New York: Plenum) p 227
[12] Kunc K and Bilz H 1976 *Solid State Commun.* **19** 1027
[13] Suzuki T, Yagi T and Akimoto S 1983 *J. Appl. Phys.* **54** 748
[14] Wettling W and Windscheif J 1984 *Solid State Commun.* **50** 33
[15] Cohen M L and Chelikowsky J R 1988 *Electronic Structure and Optical Properties of Semiconductors* ed M Cardona, P Fulde, K von Klitzing and H-J Queisser (Berlin: Springer)
[16] Kunc K and Martin R M 1983 *Ab-initio Calculation of Phonon Spectra* ed J T Devreese, V E van Doren and P E van Camp (New York: Plenum) p 65
[17] Rodriguez C O and Kunc K 1988 *J. Phys. C: Solid State Phys.* **21** 5933
[18] Churcher N, Kunc K and Heine V 1986 *J. Phys. C: Solid State Phys.* **19** 4413
[19] Cheng C, Kunc K and Heine V 1989 *Phys. Rev.* B **39** 5892
[20] Dick B G and Overhauser A W 1958 *Phys. Rev.* **112** 90
[21] Cochran W 1971 *Crit. Rev. Solid State Sci.* **2** 1, and references therein
[22] Bilz H and Kress W 1979 *Phonon Dispersion Relations in Insulators* ed M Cardona, P Fulde and H-J Queisser (Berlin: Springer) p 101
[23] Martin R M and Kunc K 1981 *Phys. Rev.* B **24** 2081